

Stable-Matching Voronoi Diagrams: Combinatorial Complexity and Algorithms

Gill Barequet

Technion – Israel Inst. of Technology, Haifa, Israel
barequet@cs.technion.ac.il

David Eppstein

University of California, Irvine, U.S.
eppstein@uci.edu

Michael T. Goodrich

University of California, Irvine, U.S.
goodrich@uci.edu

Nil Mamano

University of California, Irvine, U.S.
nmamano@uci.edu

Abstract

We study algorithms and combinatorial complexity bounds for *stable-matching Voronoi diagrams*, where a set, S , of n point sites in the plane determines a stable matching between the points in \mathbb{R}^2 and the sites in S such that (i) the points prefer sites closer to them and sites prefer points closer to them, and (ii) each site has a quota indicating the area of the set of points that can be matched to it. Thus, a stable-matching Voronoi diagram is a solution to the classic post office problem with the added (realistic) constraint that each post office has a limit on the size of its jurisdiction. Previous work provided existence and uniqueness proofs, but did not analyze its combinatorial or algorithmic complexity. We show that a stable-matching Voronoi diagram of n sites has $O(n^{2+\epsilon})$ faces and edges, for any $\epsilon > 0$, and show that this bound is almost tight by giving a family of diagrams with $\Theta(n^2)$ faces and edges. We also provide a discrete algorithm for constructing it in $O(n^3 + n^2 f(n))$ time, where $f(n)$ is the runtime of a geometric primitive that can be performed in the real-RAM model or can be approximated numerically. This is necessary, as the diagram cannot be computed exactly in an algebraic model of computation.

2012 ACM Subject Classification Theory of computation → Computational geometry

Keywords and phrases Voronoi diagram, stable matching, combinatorial complexity, lower bounds

Digital Object Identifier 10.4230/LIPIcs.ICALP.2018.89

Related Version A full version of the paper is available at [6], <https://arxiv.org/abs/1804.09411>.

Funding This work was partially supported by DARPA under agreement no. AFRL FA8750-15-2-0092 and NSF grants 1228639, 1526631, 21217322, 1618301, and 1616248. The views expressed are those of the authors and do not reflect the official policy or position of the Department of Defense or the U.S. Government.

Acknowledgements We would like to thank Nina Amenta for several helpful discussions regarding the topics of this paper. We also thank the anonymous reviewers for many useful comments.

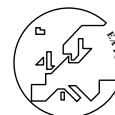


© Gill Barequet, David Eppstein, Michael T. Goodrich, and Nil Mamano;
licensed under Creative Commons License CC-BY

45th International Colloquium on Automata, Languages, and Programming (ICALP 2018).
Editors: Ioannis Chatzigiannakis, Christos Kaklamani, Dániel Marx, and Donald Sannella;
Article No. 89; pp. 89:1–89:14



Leibniz International Proceedings in Informatics
Schloss Dagstuhl – Leibniz-Zentrum für Informatik, Dagstuhl Publishing, Germany



1 Introduction

The *Voronoi diagram* is a well-known geometric structure with a broad spectrum of applications in computational geometry and other areas of Computer Science, e.g., see [3, 5, 8, 18, 20, 22, 24, 7]. The Voronoi diagram partitions the plane into regions. Given a finite set S of points, called sites, each point in the plane is assigned to the region of its closest site in S . Although the Voronoi diagram has been generalized in many ways, its standard definition specifies that each *Voronoi cell* or *region* of a site s is the set $V(s)$ defined as $\{p \in \mathbb{R}^2 \mid d(p, s) \leq d(p, s') \quad \forall s' \neq s \in S\}$, where $d(\cdot, \cdot)$ denotes the distance between two points. The properties of standard Voronoi diagrams have been thoroughly studied (e.g., see [3, 5]). For example, it is well-known that in a standard Voronoi diagram for point sites in the plane every Voronoi cell is a connected, convex polygon whose boundaries lie along perpendicular bisectors of pairs of sites.

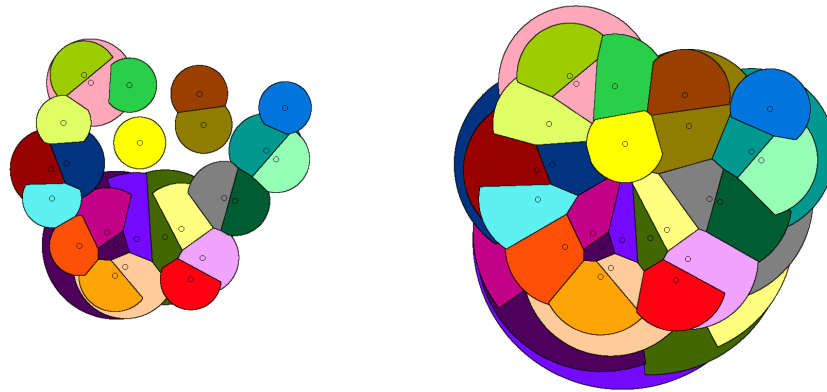
On a seemingly unrelated topic, the theory of *stable matchings* studies how to match entities in two sets, each of which has its own preferences about the elements of the other set, in a “stable” manner. It is used, for instance, to match hospitals and medical students starting their residencies [21], as well as in on-line advertisement auctions (e.g., see [2]). It was originally formulated by Gale and Shapley [12] in the context of establishing marriages between n men and n women, where each man ranks the women by preference, and the women rank the men. A matching between the men and women is *stable* if there is no *blocking pair*, that is, a man and woman who prefer each other over their assigned partners according to the matching. Gale and Shapley [12] show that a stable solution always exists for any set of preferences, and they provide an algorithm that runs in $O(n^2)$ time.

When generalized to the one-to-many case, the stable matching problem is also known as the *college admission* problem [23] and can be formulated as a matching of n students to k colleges, where each student has a preference ranking of the colleges and each college has a preference ranking of the students and a *quota* indicating how many students it can accept.

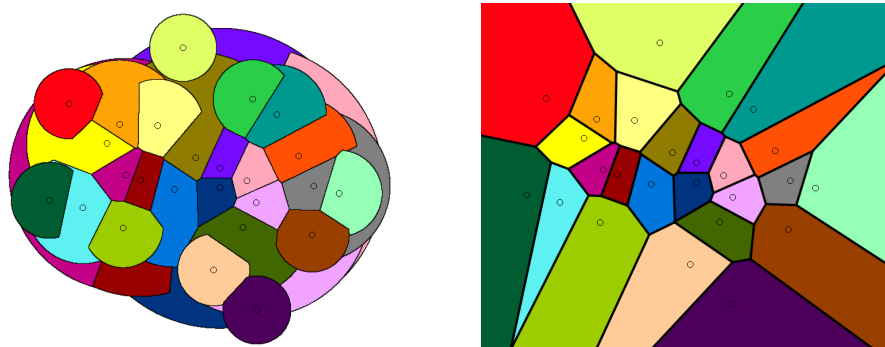
In this paper, we are interested in studying the algorithmic and combinatorial complexity of the diagrams that we call *stable-matching Voronoi diagrams*, which combine the notions of Voronoi diagrams and the one-to-many stable matching problem. These diagrams were introduced by Hoffman *et al.* [15], who provided a mathematical definition and existence and uniqueness proofs for such structures for potentially countably infinite sets of sites, but they did not study their algorithmic or combinatorial complexities. A stable-matching Voronoi diagram is defined with respect to a set of sites in \mathbb{R}^2 , which in this paper we restrict to finite sets of n distinct points, each of which has an assigned numerical *quota* (which is also known as its “*appetite*”) indicating the area of the region of points assigned to it. A preference relationship is defined in terms of distance, so that each point p in \mathbb{R}^2 prefers sites ordered by distance, from closest to farthest, and each site likewise prefers points ordered by distance. The stable-matching Voronoi diagram, then, is a partition of the plane into regions, such that (i) each site is associated with a region of area equal to its appetite, and (ii) the assignment of points to sites is stable in the sense that there is no site–point pair whose members prefer each other over their assigned matches. See Figure 1.

Formally, we can define a stable-matching Voronoi diagram for a set of sites as follows.

► **Definition 1.** Given a set S of n points (called sites) in \mathbb{R}^2 and a numerical appetite $A_s > 0$ for each $s \in S$, the *stable-matching Voronoi diagram* of S is a division of \mathbb{R}^2 into $n + 1$ regions, such that for each site $s \in S$ there is a corresponding region C_s of area A_s , and there is an extra region, C_\emptyset , for the the remaining “unmatched” points, and such that there are no blocking pairs. A blocking pair is a site $s \in S$ and a point $p \in \mathbb{R}^2$ such that (i)



■ **Figure 1** Stable-matching Voronoi diagrams for a set of 25 sites, where each site in the left diagram has an appetite of 1 and each site in the right diagram has an appetite of 2. Each color corresponds to an individual cell, which is not necessarily convex or even connected.



■ **Figure 2** A stable-matching Voronoi diagram (left) and a standard Voronoi diagram (right) for the same set of 25 sites. Each color represents a region.

$p \notin C_s$, (ii) $d(p, s) < \max \{d(p', s) \mid p' \in C_s\}$, and (iii) $p \in C_\emptyset$ or $d(p, s) < d(p, s')$, where s' is the site such that $p \in C_{s'}$.

Figure 2 shows a side-by-side comparison of the standard and stable-matching Voronoi diagrams. Note that the standard Voronoi diagram is stable in the same sense as the stable-matching Voronoi diagram. This is because, by definition, every point is matched to its first choice among the sites, so there can be no blocking pairs. Thus, standard Voronoi diagram can be seen as a stable-matching Voronoi diagram with infinite appetites, in the following sense: for any point p in \mathbb{R}^2 , for sufficiently large appetites for all the sites, p will belong to the region of the same site in the standard and stable-matching Voronoi diagrams.

In this paper, we focus on the case where all the appetites are equal, i.e., $A_s = A$, for some $A > 0$, but our results are easily adapted to the general case of arbitrary positive appetites.

A stable-matching Voronoi diagram solves the *post office* problem [19], of assigning points to their closest post office, under the (realistic) real-world assumption that each post office has an upper bound on the size of its jurisdiction. Such notions may also be useful for political districting, where sites could, for instance, represent polling stations, and appetites could represent their capacities. In this context, the distance preferences for a stable-matching Voronoi diagram might determine a type of “compactness” that avoids the strange regions

that are the subjects of recent court cases involving gerrymandering. Nevertheless, depending on the appetites and sites, the regions for sites in a stable-matching Voronoi diagram are not necessarily convex or even connected (e.g., see Figure 1). Thus, we are interested in this paper in characterizing the worst-case combinatorial complexity of such diagrams as well as finding an efficient algorithm for constructing them.

Previous Related Work. There are large volumes of work on the topics of Voronoi diagrams and stable matchings; hence, we refer the interested reader to surveys or books on the subjects (e.g., see [3, 5, 14, 16]).

A generalization of Voronoi diagram of particular relevance are *power diagrams*, where a weight associated to each site indicates how strongly the site draws the points in its neighborhood. Aurenhammer *et al.* [4] showed that, given a quota for each site, it is always possible to find weights for the sites such that, in the power diagram, the region of each site will have area equal to its prescribed quota. Thus, both stable-matching Voronoi diagrams and power diagrams are Voronoi-like diagrams with predetermined region sizes. Power diagrams minimize the total square distance between the sites and their associated points, while stable-matching Voronoi diagrams result in a stable matching.

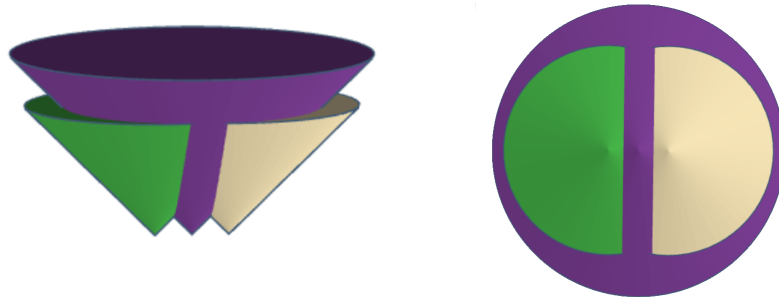
As mentioned above, Hoffman *et al.* [15] gave definitions and existence and uniqueness proofs for the structures we call stable-matching Voronoi diagrams, albeit for potentially countably infinite sets of point sites. Rather than giving a discrete algorithm for constructing such diagrams, however, they described a continuous process that results in the stable-matching Voronoi diagram: Start growing a circle from all the sites at the same time and at the same rate, matching the sites with all the points encountered by the circles that are not matched yet – when a site fulfills its appetite, its circle stops growing. The process ends when all the circles have stopped growing. Of course, such a continuous process could be approximated numerically, but it is not an effective discrete algorithm, which is one of the interests of the present paper.

In other previous work, Eppstein *et al.* [10] studied the problem of constructing a stable-matching Voronoi diagram in a discrete $n \times n$ grid setting, where both sites and points are pixels. Later, Eppstein *et al.* [9] considered a related stable-matching problem in the context of planar graphs and road networks. In these two previous works, the entities analogous to sites and points are either pixels or vertices; hence, these previous algorithms did not encounter the algorithmic and combinatorial challenges raised by stable-matching Voronoi diagrams for sites and points in the plane.

Our Contributions. In Section 2, we give a geometric interpretation of stable-matching Voronoi diagrams as the lower envelope of a set of cones, and discuss some basic properties of stable-matching Voronoi diagrams.

In Section 3, we give an $O(n^{2+\epsilon})$ upper bound, for any $\epsilon > 0$, and an $\Omega(n^2)$ lower bound for the number of faces and edges of a stable-matching Voronoi diagrams in the worst case, where n is the number of sites.

In Section 4, we show that stable-matching Voronoi diagrams cannot be computed exactly in an algebraic model of computation. In light of this, we provide a discrete algorithm for constructing them that runs in $O(n^3 + n^2 f(n))$ time, where $f(n)$ is the runtime of a geometric primitive (which we identify) that encapsulates this difficulty. The geometric primitive can be computed in the real-RAM model or can be approximated numerically. We conclude in Section 5.



■ **Figure 3** View of a stable-matching Voronoi diagram of 3 sites as the lower envelope of a set of cones.

2 The Geometry of Stable-Matching Voronoi Diagrams

As is now well-known, a (2-dimensional) Voronoi diagram can be viewed as a lower envelope of cones in 3 dimensions, as follows [11]. Suppose that the sites are embedded in the plane $z = 0$. That is, we map each site $s = (x_s, y_s)$ to the 3-dimensional point $(x_s, y_s, 0)$. Then, we draw one cone for each site, with the site as the apex, and growing to $+\infty$ all with the same slope. If we then view the cones from below, i.e., from $z = -\infty$ towards $z = +\infty$, the part of the cone of each site that we see corresponds to the Voronoi cell of the site. This is because two such cones intersect at points that are equally distant to the two apices. As a result, the xy -projection of their intersection corresponds to the perpendicular bisector of the apices, and the boundaries of the Voronoi cells in the Voronoi diagram are determined by the perpendicular bisectors with neighboring sites.

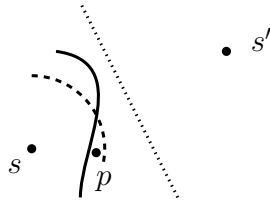
Similarly, a stable-matching Voronoi diagram can also be viewed as the lower envelope of a set of cones, where, instead of extending to $+\infty$, cones are cut off at a finite height (which is a potentially different height for each cone, even if the associated sites have the same appetite). This system of cones can be generated by a dynamic process that begins with cones of height zero and then grows them all at the same rate, halting the growth of each cone as soon as its area in the lower envelope reaches its appetite (see Figure 3).

A stable-matching Voronoi diagram consists of three types of elements:

- A *face* is a maximal, closed, connected subset of a stable cell. The stable cells can be disconnected, that is, a cell can have more than one face. There is also one or more *empty faces*, which are maximal connected regions not assigned to any site. One of the empty faces is the *external face*, which is the only face with infinite area.
- An *edge* is a maximal line segment or circular arc on the boundary of two faces. We call the two types of edges *straight* and *curved edges*, respectively. For curved edges, we distinguish between its incident convex face (the one inside the circle along which the edge lies) and its incident concave face.
- A *vertex* is a point shared by more than one edge. Generally, edges end at vertices, but curved edges may have no endpoints when they form a complete circle. This situation arises when the region of a site is isolated from other sites.

For a given appetite, shared by all the sites, we say that sites are not in general position if two curved boundaries of the stable-matching Voronoi diagram touch at a point, p , that is not an endpoint (e.g., two circles of radius 1 with centers 2 units apart) and, hence, for those curved edges, the concave face is the same at both sides of p . In this special case, we consider that the curved edges end at the vertex p .

In order to study the topology of the distance-stable Voronoi diagram, let the *bounding*



■ **Figure 4** Illustration of the setting in the proof of Lemma 2. It shows the perpendicular bisector of two sites s and s' (as a dotted line), the boundary of the bounding disk, B_s , of s (as a dashed circular arc), and a hypothetical boundary between the regions of sites s and s' (as a solid curve). In this setting, s and p would be a blocking pair.

disk, B_s , of a site, s , be the smallest (closed) disk centered at s that contains the stable cell of s . The bounding disks arise in the topology of the diagram due to the following lemma:

► **Lemma 2.** *If part of the boundary between a face of site s and a face of site s' lies in the half-plane closer to s than to s' , then that part of the boundary must lie along the boundary of the bounding disk B_s of s , and the convex face must belong to s .*

Proof. The boundary between the faces of s and s' cannot lie outside of B_s , by definition of the bounding disk. If the boundary is in the half-plane closer to s , then it also cannot be in the interior of B_s , because then there would exist a point p inside B_s and in the half-plane closer to s , but matched to s' (see Figure 4). In such a situation, s and p would be a blocking pair: s prefers p to the point(s) matched to it along B_s , and p prefers s to s' . ◀

► **Lemma 3.** *The union of non-empty faces of the diagram is the union of the bounding disks of all the sites.*

Proof. For any site s , all the points inside the bounding disk of s must be matched. Otherwise, there would be a point, say, p , not matched to anyone but closer to s than points actually matched to s (along the boundary of B_s), which would be unstable, as p and s would be a blocking pair. Moreover, points outside of all the bounding disks cannot be matched to anyone, by definition of the bounding disks. ◀

► **Lemma 4** (Characterization of edges).

1. *A straight edge separating faces of sites s and s' can only lie along the perpendicular bisector of s and s' .*
2. *A curved edge whose convex face belongs to site s lies along the boundary of the bounding disk of s . Moreover, if the concave face belongs to a site s' , the edge must be contained in the half-plane closer to s than s' .*
3. *Empty faces can only be concave faces of curved edges.*

Proof. Claims (1) and (2) are consequences of Lemma 2, and Claim (3) is a consequence of Lemma 3. ◀

Generally, every site has at least one curved edge. The only case where that may not happen is when the appetite of a site is exactly the same as the area of its Voronoi cell.

3 Combinatorial Complexity

3.1 An Upper Bound on the Number of Faces

As mentioned in Section 2, a stable-matching Voronoi diagram can be viewed as the lower envelope of a set of cones. The study of *Davenport-Schinzel sequences* has yielded results that characterize the combinatorial complexity of the lower envelope of certain sets of functions (e.g., see Sharir and Agarwal [1]), including cones.

Formally, the *lower envelope* (also called *minimization diagram*) of a set of bivariate continuous functions $F = \{f_1(x, y), \dots, f_n(x, y)\}$ is the function $E_F(x, y) = \min_{1 \leq i \leq n} f_i(x, y)$. The lower envelope of F partitions the plane into maximal connected regions such that E_F is attained by a single function f_i (or by no function at all). The *combinatorial complexity* of the lower envelope E_F , denoted $K(F)$, is the number of maximal connected regions of E_F . To prove our upper bound, we use the following result:

► **Lemma 5.** *Sharir and Agarwal [1, p. 191] The combinatorial complexity $K(F)$ of the lower envelope of a collection F of n (partially defined) functions that satisfy the assumptions below¹ is $O(n^{2+\varepsilon})$, for any $\varepsilon > 0$.*

- Each $f_i \in F$ is a portion of an algebraic surface of the form $P(x_1, \dots, x_d) = 0$, for some polynomial P of constant maximum degree.
- The vertical projection of each $f_i \in F$ onto the xy -plane is a planar region bounded by a constant number of algebraic arcs of constant maximum degree.

► **Corollary 6.** *A stable-matching Voronoi diagram for n sites has $O(n^{2+\varepsilon})$ faces, for any $\varepsilon > 0$.*

Proof. It is clear that the finite, “upside-down” cones whose lower envelope forms the stable-matching Voronoi diagram of a set of sites satisfy the assumptions from Lemma 5. In particular, their projection onto the xy -plane are disks. Note that the bound still applies if we include the empty faces, as the assumptions still hold if we add an extra bivariate function $f_{n+1}(x, y) = z^*$, where z^* is any value higher than the height of any cone (i.e., f_{n+1} is a plane that “hovers” over the cones). Such a function would have a face in the lower envelope for each empty face in the stable-matching Voronoi diagram. ◀

3.2 An Upper bound on the Number of Edges and Vertices

Euler’s formula relates the number of faces in a planar graph with the number of vertices and edges. By viewing the stable-matching Voronoi diagram as a graph, we can use Euler’s formula to prove that the $O(n^{2+\varepsilon})$ upper bound also applies to the number of edges and vertices. In order to do so, we need the following lemma, for which we defer the proof to the full version of the paper [6] due to space constraints.

► **Lemma 7.** *The average degree is at least 2.25.*

In this section (Lemmas 7 and 8), we assume that sites are in general position (as defined in Section 2). However, note that non-general-position constructions cannot yield the worst-case complexity. This is because if two curved boundaries coincide exactly at a point that is not an endpoint, we can perturb slightly the site locations to move them a little closer, which creates a new vertex and edge.

¹ The theorem, as stated in [1] (Theorem 7.7), includes some additional assumptions, but then shows that they are not essential.

► **Lemma 8.** *Let V, E and F be the number of vertices, edges, and faces of the stable-matching Voronoi diagram of a set of sites S . Then, $V \leq 8F - 16$ and $E \leq 9F - 18$.*

Proof. For this proof, suppose that there are no curved edges that form a full circle. Note that the presence of such edges can only reduce the number of vertices and edges, as for each such edge there is a site with a single edge and no vertices.

Without such edges, the vertices and edges of the stable-matching Voronoi diagram form a planar graph, and V, E, F are the number of vertices, edges, and faces of this graph, respectively. Moreover, let C be the number of connected components. Due to Euler's formula for planar graphs, we have $F = E - V + C + 1$, and thus $F \geq E - V + 2$. Moreover, by Lemma 7, the sum of degrees is at least $2.25V$, so $2E \geq 2.25V$. Combining the two relations above, we have $V \leq 8F - 16$ and $E \leq 9F - 18$. ◀

We conclude by stating the main theorem of this section, which is a combination of Corollary 6 and Lemma 8:

► **Theorem 9.** *A stable-matching Voronoi diagram for n sites has $O(n^{2+\varepsilon})$ faces, vertices, and edges, for any $\varepsilon > 0$.*

3.3 Lower Bound

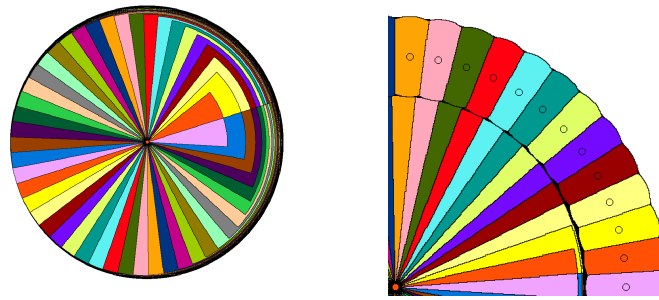
► **Lemma 10.** *A stable-matching Voronoi diagram for n sites has $\Omega(n^2)$ faces in the worst case.*

Proof. Let $m = \lfloor n/2 \rfloor$. We will construct a diagram in two steps, first placing m sites, and then m more. If n is odd, the remaining site can be placed anywhere in the plane that does not intersect with the others.

First, consider the stable-matching Voronoi diagram of m sites, each with appetite one, placed evenly on a circle with very small radius ε_1 . Then, perturb them slightly so that the circular angle between two specific sites s, s' is slightly bigger than the rest: $2\pi/n + \varepsilon_2$, while the angle between any other pair of sites is $2\pi/n - \varepsilon_2/(n-1)$, again for a very small $\varepsilon_2 > 0$. As a result, the standard Voronoi regions of the sites are infinite angular regions, but those of s and s' are slightly wider than those of the remaining sites.

The result is a diagram such as the one in Figure 5, Left. To see this, consider the circle-growing method from [15] described in Section 1. All the sites start growing their region as a circle, which quickly overlap with the other sites. As a result, each site is constrained to grow in the angular region corresponding to its own Voronoi region. Since s and s' have wider angles, they fill their appetite slightly before the rest, which grow at the same rate. After s and s' stop growing, the angular regions “available” to grow for the sites adjacent to s and s' increases to include the Voronoi regions of s and s' . Since now the neighbors of s and s' grow their regions faster than the rest, they also fill their appetite before the remaining sites. This process continues so that, in the end, one half of the sites “wrap” around the circle all the way to the Voronoi region of s , and the other half wrap around to the Voronoi region of s' .

As a result, we get m almost equal-area wedges surrounded by $O(m)$ very thin circular strips. We can choose ε_2 to set exactly how far the stable cell of s and s' reach, and therefore the overall width of all the circular strips. Then, we can set ε_1 small enough to ensure that all the circular strips wrap around the entire circle. Note that, as ε_1 approaches 0, the entire diagram approaches a circle of area m where all the sites want to grow equally far in every angular region.



■ **Figure 5 Left:** A stable-matching Voronoi diagram of 50 sites situated around a small circle with the perturbed angles. **Right:** Zoom of a section of the stable-matching Voronoi diagram after adding 50 more sites situated evenly along a bigger, concentric circle (and with a smaller ε_2 than in the left figure).

Then, we place the remaining m sites evenly along an exterior concentric circle (see Figure 5, Right), and at a distance so that each outer site will have its appetite satisfied only by cutting into the circular strip. Because the wedges of the sites along the interior circle are very thin, the outer sites are closer to the circular strips than the inner sites; hence, each one can “steal” points in the strips away from the inner sites (which then need to get additional points from beyond the regions of the outer sites). At least half of the strips are as long as half the circle, and hence they get each broken into $\Theta(m)$ faces. Therefore, the circular strips are collectively broken into a total of $\Theta(m^2) = \Theta(n^2)$ faces. ◀

4 Paint-by-Numbers Algorithm

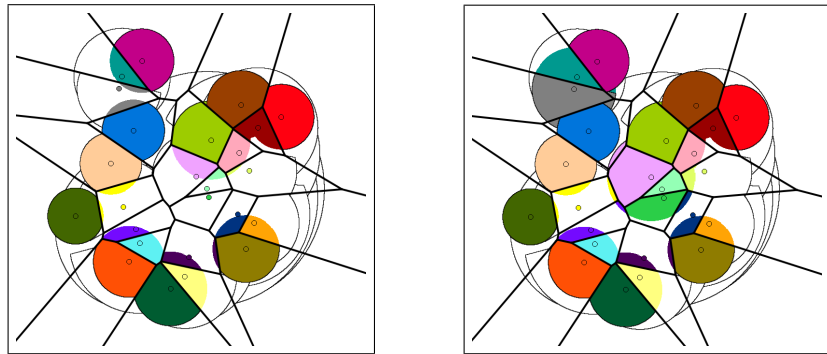
There are two similar incremental approaches to construct the stable matching Voronoi-diagram by processing sites one at a time. One option is to add the region of a site at each step. The other option, which we describe in this section, is to add the bounding disk of a site at each step, partitioned according to the diagram. In both cases, the key is to process the sites by increasing radii of their bounding disks. The major challenge lies in finding the bounding disks, which we will encapsulate in a geometric primitive (Definition 16). We focus on the second approach because the needed geometric primitive is simpler.

Finding the sites by increasing radii of their bounding disks might seem impossible at first, since, when our algorithm starts, the radii of the bounding disks for almost all the sites will, in general, be unknown. Nevertheless, as our algorithm progresses, we can know the radius of the smallest bounding disk of the sites remaining to be processed. Thus, at each iteration, we find a site, s , with smallest-radius bounding disk, B_s , from among the remaining unprocessed sites. Then, reminiscent of a “paint-by-numbers” drawing, we add to the matching all the unmatched points in B_s , using the boundary of B_s and the cells of a standard Voronoi diagram of the remaining unprocessed sites as the guides of how to “color” points. Figure 6 shows two snapshots of the intermediate steps of our paint-by-numbers algorithm. Suppose, then, that we are given a set, S , of n sites in the plane, each with appetite A .

Our algorithm is based on the following result. For a site s , let r_s be the radius of its bounding circle, B_s .

▶ **Lemma 11.** *If $r_s \leq r_{s'}$, no point p inside B_s such that $d(p, s') < d(p, s)$ is matched to s .*

Proof. Any such point p prefers s' to s . Moreover, we have that $d(p, s') < d(p, s) \leq r_s \leq r_{s'}$.



■ **Figure 6** Partial matching done by the incremental paint-by-numbers algorithm after 10 iterations (left) and 12 iterations (right). The sites with the 11th and 12th smallest bounding disks are the gray site in the top-left and the light violet site in the center, respectively. In each case, the edges of the standard Voronoi diagram and the stable-matching Voronoi diagram are overlaid in thick and thin black lines, respectively.

Thus, s' prefers p to the points matched to s' along the boundary of $B_{s'}$. Hence, if p was matched to s , p and s' would be a blocking pair. ◀

► **Corollary 12.** *The stable cell of a site s is contained in $V(s)$, the Voronoi cell of s in the standard Voronoi diagram of the subset of sites whose bounding disks have radius at least r_s .*

Proof. The stable cell of s is contained in B_s , but any point in B_s that is not in $V(s)$ is closer to a site other than s whose bounding disk has radius at least r_s . According to Lemma 11, any such point cannot be matched to s . ◀

Our incremental paint-by-numbers algorithm proceeds as follows:

1. Initialize $X = S$ as the set of sites remaining to be processed and $X^* = \emptyset$ as the set of sites that have already been processed. Moreover, for each site s , initialize its partially constructed stable cell C_s as empty, and its remaining appetite, $A_s = A$.
2. Compute a standard Voronoi diagram, V , of the sites in X .
3. Repeat until X is empty:
 - a. For each site s in X , calculate r_s , the current estimate for the radius of the bounding disk for s , as follows; r_s is the radius such that the area of the subset of $V(s)$ (the Voronoi cell of s in V) within that radius of s , excluding the bounding disks of sites in X^* , equals A_s .
 - b. Choose a site s whose radius r_s is minimum. (By Corollary 12, r_s is the radius of B_s .)
 - c. Compute $B_s^* = B_s \setminus \{B_{s'} \mid s' \in X^*\}$, the bounding disk of s minus the already-matched bounding disks.
 - d. Match the points in B_s^* : for each site s' in X (including s), add to $C_{s'}$ the (possibly empty) intersection $B_s^* \cap V(s')$, and decrease the appetite, $A_{s'}$, of s' , by the area of this intersection.
 - e. Move s from X to X^* , and remove s from V .

► **Theorem 13.** *The stable-matching Voronoi diagram of a set, S , of n sites can be computed in the real-RAM model in $O(n^3)$ time plus $O(n^2)$ calls to a geometric primitive that has input complexity $O(n)$.*

Let us provide a proof of Theorem 13, beginning with the correctness of our paint-by-numbers algorithm.

► **Lemma 14** (Correctness). *The paint-by-numbers algorithm correctly computes the stable-matching Voronoi diagram of a set, S , of n sites.*

Proof. The algorithm matches all the points inside the bounding disks of the sites, and only those. Therefore, it matches precisely the points in the stable-matching Voronoi diagram (Lemma 3). Note that, when finding the site s in X with the smallest bounding disk, we can rely on Corollary 12, which says that the stable cell of s must be contained in $V(s)$.

It remains to be seen that the matching of the points in each bounding disk is correct. Consider the iteration where we process the site s , and let p be a point in B_s^* and in the inside of $V(s')$ (such that $s' \neq s$). The algorithm matches p to s' , so we need to see that p belongs to the stable cell of s' . On the one hand, p does not belong to the stable cell of any site in X^* because p lies outside their bounding disks. Moreover, by virtue of being in $V(s')$, p prefers s' to any other site in X . On the other hand, $d(p, s') < d(p, s) \leq r_s \leq r_{s'}$, so s' also prefers p to some of its matched points. Hence, if p and s' were not matched to each other, they would be a blocking pair.

Similarly, in the case where p is in the inside of $V(s)$, the algorithm matches p to s and p belongs in the stable cell of s . ◀

Finding the radii r_s (Step 3a) is the most challenging step in our algorithm. In fact, Observation 15, which we prove in the full version of the paper [6], speaks to its difficulty.

► **Observation 15.** For infinitely-many sets of sites in general position and with algebraic coordinates, the radius of some of the sites' bounding disks cannot be computed exactly in an algebraic model of computation.

To circumvent this problem, we encapsulate the difficulty in computing each r_s analytically in a geometric primitive that can be performed in the real-RAM model or approximated numerically in an algebraic model of computation. That is, for the sake of the algorithm description, we assume the existence of a black-box function that allows us to compute the following geometric primitive.

► **Definition 16** (Geometric primitive). Given a convex polygon P , a point s in P , an appetite A , and a set C of disks, return the radius r (if it exists) such that A equals the area of the intersection of $P \setminus C$ and a disk centered at s with radius r .

In the context of our algorithm, the point s is a site in X , the appetite, A , is the remaining appetite, A_s , of s , the polygon P is the Voronoi cell $V(s)$, and the set of disks C is the set of bounding disks of the sites in X^* . Note that such a primitive could be approximated numerically to arbitrary precision, e.g., with a binary search and a simple decision algorithm.

Another detail for our algorithm that we need to spell out is how to maintain the partially constructed cell C_s of each site s . The structure C_s consists of a set of disjoint regions, each of which is delimited by straight and curved edges. Note that the straight edges are part of actual edges of the stable cell of s , as the other side is already matched to some other site. However, the convex curved edges (edges such that the convex face belongs to C_s) found before the iteration of s are not part of edges in the stable cell of s , as they lie along the boundary of the bounding disks of sites other than s (see, e.g., the gray regions in Figure 6, Left). Only at the iteration of s we find the proper convex curved edges of the stable cell of s . The points on the concave face of one of these “fake” convex edges of C_s must also belong to C_s . In some posterior iteration, when the region in the concave face is matched as part of another bounding disk $B_{s'}^*$, the region of $B_{s'}^*$ added to C_s will have a matching concave edge. Thus, when we add a concave edge to C_s , we look for a corresponding convex edge in C_s ,

and if we find one, we “glue” them together, by removing the overlapping part. Similarly, we also merge straight edges sharing an endpoint.

Let us turn, then, to the analysis of the running time of the paint-by-numbers algorithm. For the number of calls to the geometric primitive, note that there are n iterations, and at each iteration we call the geometric primitive $O(n)$ times. The Voronoi diagram V has $O(n)$ edges and there are $O(n)$ already-matched disks, so the input of each call has $O(n)$ size. That is, we make $O(n^2)$ calls to the geometric primitive, each of which has combinatorial complexity $O(n)$.

The remaining steps of each iteration all can be done in $O(n^2)$ time, by the following observations:

1. The running time of Step 3b is clearly $O(n)$.
2. The combinatorial complexity of the standard Voronoi diagram, V , is $O(n)$ and it can be initially computed (Step 2) in $O(n \log n)$ time (e.g., see [3, 5]) and updated after the removal of any point site (Step 3e) in $O(n)$ time [13].
3. By the previous observation (2), for any single bounding disk, B_s , chosen in an iteration of our algorithm, B_s has an intersection with V that has combinatorial complexity $O(n)$.
4. The union of the set of bounding disks for the points in X^* has combinatorial complexity $O(n)$ [17, 1].
5. By the previous observation (4), for any single bounding disk, B_s , chosen in an iteration of our algorithm, the combinatorial complexity of B_s^* , that is, B_s minus all the bounding disks for sites in X^* , is $O(n)$. Thus, the running time of Step 3c in any iteration is $O(n)$.
6. Combining the above observations 3 and 5, the combinatorial complexity of the pieces of B_s^* intersecting V has combinatorial complexity $O(n^2)$. Thus, the running time of Step 3d in any iteration is $O(n^2)$.

Therefore, the total running time of our paint-by-numbers algorithm is $O(n^3 + n^2 f(n))$, where $f(n)$ is the running time of the geometric primitive defined above. This completes the proof of Theorem 13.

5 Conclusions

We have studied stable-matching Voronoi diagrams, providing characterizations of their combinatorial complexity and a first discrete algorithm for constructing them. The fact that (i) both the standard and stable-matching Voronoi diagrams share the stability property, in terms of preferences based on distances, and that (ii) both have similar geometric constructions in terms of the lower envelopes of cones, supports the idea that stable-matching Voronoi diagrams are a natural generalization of the standard Voronoi diagram to sized-constrained regions. However, this comes at the cost of convexity and connectivity; indeed, we have shown that a stable-matching Voronoi diagram may have $O(n^{2+\varepsilon})$ faces and edges, for any $\varepsilon > 0$. It would be interesting to see if this bound can be brought down to $O(n^2)$, which would make it tight. Constructing a stable-matching Voronoi diagram is also more computationally challenging than the construction of a standard Voronoi diagram. We have given a first algorithm which runs in $O(n^3 + n^2 f(n))$ -time, where $f(n)$ is the runtime of a geometric primitive that we defined to encapsulate the computations that cannot be carried analytically. While such primitives cannot be avoided, a step forward from our algorithm would be one that relies only in primitives with constant-sized inputs.

References

- 1 P. K. Agarwal and Micha Sharir. Davenport–Schinzel Sequences and Their Geometric Applications. Technical Report DUKE–TR–1995–21, Duke University, Durham, NC, USA, 1995.
- 2 Gagan Aggarwal, S. Muthukrishnan, Dávid Pál, and Martin Pál. General auction mechanism for search advertising. In *18th Int. Conf. on the World Wide Web (WWW)*, pages 241–250. ACM, 2009. doi:10.1145/1526709.1526742.
- 3 Franz Aurenhammer. Voronoi diagrams—A survey of a fundamental geometric data structure. *ACM Computing Surveys*, 23(3):345–405, 1991. doi:10.1145/116873.116880.
- 4 Franz Aurenhammer, Friedrich Hoffmann, and Boris Aronov. Minkowski-type theorems and least-squares clustering. *Algorithmica*, 20(1):61–76, 1998. doi:10.1007/PL00009187.
- 5 Franz Aurenhammer, Rolf Klein, and Der-Tsai Lee. *Voronoi Diagrams and Delaunay Triangulations*. World Scientific, 2013.
- 6 Gill Barequet, David Eppstein, Michael T. Goodrich, and Nil Mamano. Stable-Matching Voronoi Diagrams: Combinatorial Complexity and Algorithms. Electronic preprint arXiv:1804.09411, 2018.
- 7 Priyadarshi Bhattacharya and Marina L. Gavrilova. Roadmap-based path planning – Using the Voronoi diagram for a clearance-based shortest path. *IEEE Robotics Automation Magazine*, 15(2):58–66, 2008. doi:10.1109/MRA.2008.921540.
- 8 Jonathan W. Brandt and V. Ralph Algazi. Continuous skeleton computation by Voronoi diagram. *CVGIP: Image Understanding*, 55(3):329–338, 1992. doi:10.1016/1049-9660(92)90030-7.
- 9 David Eppstein, Michael T. Goodrich, Doruk Korkmaz, and Nil Mamano. Defining equitable geographic districts in road networks via stable matching. In *25th ACM SIGSPATIAL Int. Conf. on Advances in Geographic Information Systems*, 2017.
- 10 David Eppstein, Michael T. Goodrich, and Nil Mamano. Algorithms for stable matching and clustering in a grid. In *18th Int. Workshop on Combinatorial Image Analysis (IWCIA)*, volume 10256 of *LNCS*, pages 117–131. Springer, 2017. doi:10.1007/978-3-319-59108-7_10.
- 11 Steven Fortune. A sweepline algorithm for Voronoi diagrams. *Algorithmica*, 2(2):153–174, 1987. doi:10.1007/BF01840357.
- 12 David Gale and Lloyd S. Shapley. College admissions and the stability of marriage. *The American Mathematical Monthly*, 69(1):9–15, 1962. doi:10.2307/2312726.
- 13 Ihor G. Gowda, David G. Kirkpatrick, Der Tsai Lee, and Amnon Naamad. Dynamic Voronoi diagrams. *IEEE Transactions on Information Theory*, 29(5):724–731, September 1983. doi:10.1109/TIT.1983.1056738.
- 14 Dan Gusfield and Robert W. Irving. *The Stable Marriage Problem: Structure and Algorithms*. MIT Press, Cambridge, MA, USA, 1989.
- 15 Christopher Hoffman, Alexander E. Holroyd, and Yuval Peres. A stable marriage of Poisson and Lebesgue. *Annals of Probability*, 34(4):1241–1272, 2006. doi:10.1214/009117906000000098.
- 16 Kazuo Iwama and Shuichi Miyazaki. A survey of the stable marriage problem and its variants. In *IEEE Int. Conf. on Informatics Education and Research for Knowledge-Circulating Society (ICKS)*, pages 131–136, 2008. doi:10.1109/ICKS.2008.7.
- 17 Klara Kedem, Ron Livné, János Pach, and Micha Sharir. On the union of Jordan regions and collision-free translational motion amidst polygonal obstacles. *Discrete Comput. Geom.*, 1(1):59–71, 1986. doi:10.1007/BF02187683.
- 18 Koichi Kise, Akinori Sato, and Motoi Iwata. Segmentation of page images using the area Voronoi diagram. *Computer Vision and Image Understanding*, 70(3):370–382, 1998. doi:10.1006/cviu.1998.0684.

- 19 Donald E. Knuth. *The Art of Computer Programming, Vol. 3: Sorting and Searching*. Addison-Wesley, Reading, MA, 2nd edition, 1998.
- 20 Seapahn Meguerdichian, Farinaz Koushanfar, Gang Qu, and Miodrag Potkonjak. Exposure in wireless ad-hoc sensor networks. In *7th Int. Conf. on Mobile Computing and Networking (MobiCom)*, pages 139–150. ACM, 2001. doi:10.1145/381677.381691.
- 21 National Resident Matching Program, 2017. URL: <http://www.nrmp.org>.
- 22 Martin Petřek, Pavlína Košinová, Jaroslav Koča, and Michal Otyepka. MOLE: A Voronoi diagram-based explorer of molecular channels, pores, and tunnels. *Structure*, 15(11):1357–1363, 2007. doi:10.1016/j.str.2007.10.007.
- 23 Alvin E. Roth and Marilda Sotomayor. The college admissions problem revisited. *Econometrica*, 57(3):559–570, 1989. doi:10.2307/1911052.
- 24 Ivan Stojmenović, Anand Prakash Ruhil, and D. K. Lobiyal. Voronoi diagram and convex hull based geocasting and routing in wireless networks. *Wireless Communications and Mobile Computing*, 6(2):247–258, 2006. doi:10.1002/wcm.384.